Evaluation of the hygroscopic behavior of aerosols over São Paulo: one-day case study

Patrícia Ferrini Rodrigues[a], Eduardo Landulfo[a], Fábio Juliano da Silva Lopes[a,b], Renata Facundes da Costa[a], María Jose Granados-Muñoz[c,d], Juan Luis Guerrero-Rascado[c,d]

[a]Instituto de Pesquisas Energéticas e Nucleares, IPEN/CNEN-SP, Av Prof. Lineu Prestes, 2242, São Paulo, Brazil;
[b]Universidade de São Paulo, Instituto de Astronomia, Geofísica e Ciências Atmosféricas, Rua do Matão, 1226, Cidade Universitária, São Paulo, Brasil;
[c]Instituto Interuniversitario de Investigacion del Sistema Tierra en Andalucía (IISTA-CEAMA), Av. del Mediterráneo, 18006, Granada, España;
[d]Dpto. Física Aplicada, Universidad de Granada, Fuentenueva s/n, Granada, España;

ABSTRACT

Aerosol hygroscopicity is a property that reveals the ability of an aerosol particle to grow under increasing values of relative humidity. The hygroscopic behavior has a significant effect on radiative properties of aerosols, and therefore on cloud formation, aerosol-cloud interaction and, consequently, on the Earth's climate. In this work, a Raman LIDAR is used to determine the hygroscopic growth factor $f_\beta(RH)$ under unperturbed, ambient atmospheric conditions in a well-mixed boundary layer in São Paulo metropolitan city.

To this aim, the water vapor mixing ratio (required to derive the hygroscopic growth factor) was independently obtained by radiosoundings and Raman LIDAR (after the corresponding calibration using radiosoundings), and the hygroscopic growth factor was determined using both instruments.

There is a good agreement between the values obtained by the LIDAR and by the radiosoundings, although many uncertainties still remain in the hygroscopic growth factor determination. It suggests that the Raman LIDAR method can provide useful measurements of the dependence of aerosol optical properties on relative humidity and under conditions closer to saturation.

Keywords: Raman LIDAR, Water Vapor, hygroscopic growth, radiosounding

1. INTRODUCTION

The size increase of aerosol due the water uptake has important effects on direct radiation scattering (direct effect), but it has also influences on indirect effects, related to the capacity of this aerosol population to act as CCN (cloud condensation nucleai) - i.e. the ability of an aerosol particle to grow its liquid water content and form cloud droplets.[1] As the relative humidity (RH) of the environment increases, condensation of water vapor may occur over aerosols, depending on their physical, chemical and thermodynamical properties. This phenomenon leads to an increase of the particle size (hygroscopic growth) and consequently causes changes in the particle refractive index and other particle optical properties.[2] Therefore, significant variations in the backscattered signal detected with a LIDAR are expected when changes in RH are observed. This is particularly true for high RH values, where hygroscopic growth of aerosols is more pronounced.[3]

Numerous experimental studies of aerosol scattering and relative humidity have been performed in laboratory using a well-known aerosol population in terms of chemical nature.[4] *In situ* experiments using nephelometers were also useful to study of this property.[5,6]

The remote sensing technique using LIDAR has several advantages over other methods on measuring hygroscopic growth. Foremost, the fact that this remote sensing system is able to measure changes in backscattering under

Further author information: Send correspondence to Patrícia Ferrini Rodrigues.
E-mail: patricia.ferrini.rodrigues@usp.br

Lidar Technologies, Techniques, and Measurements for Atmospheric Remote Sensing X, edited by Upendra N. Singh, Gelsomina Pappalardo, Proc. of SPIE Vol. 9246, 92460G
 · doi: 10.1117/12.2067469

unperturbed atmospheric conditions, besides the fact that the range of measurements can be extended to very close to saturation,[7] as the traditional methods using nephelometers can not expose dry samples of particles to a relative humidity over 85% (the region where particles experience their most noticeable growth). The main disadvantage is that the aerosol population can not be controlled and specific atmospheric conditions must be present, namely, when the atmosphere is well mixed and there is the same aerosol population at least in a portion of the profile where a widely change in RH can be observed. These conditions ensure that any changes in backscattering are due to water uptake by the particles.[7]

2. METHODOLOGY

2.1 Instrumentation

2.1.1 System Setup

The LIDAR system used in this study is called MSP-Lidar I (LIDAR do Município de São Paulo) and belongs to the Latin America LIDAR Network (LALINET - *http* : *//lalinet.org/*). It is a multiwavelength Raman LIDAR operated by the Lasers Environmental Applications Research Group at the Center for Lasers and Applications (CLA), Nuclear and Energy Research Institute (IPEN) in São Paulo ($-23°$ 56' S, 46°74' W, 740 m above sea level). It is a monoestatic coaxial system, pointed vertically to the zenith and using a commercialized Nd:YAG laser by Quantel, model Brilliant B, with a fundamental wavelength of 1064 nm, and generating second and third harmonics, 532 nm and 355 nm, respectively, at a repetition rate of 10 Hz. The output energy per pulse is 850 mJ for 1064 nm, 400 mJ for 532 nm and 230 mJ for 355 nm. The pulse duration is 6 ± 2 ns.

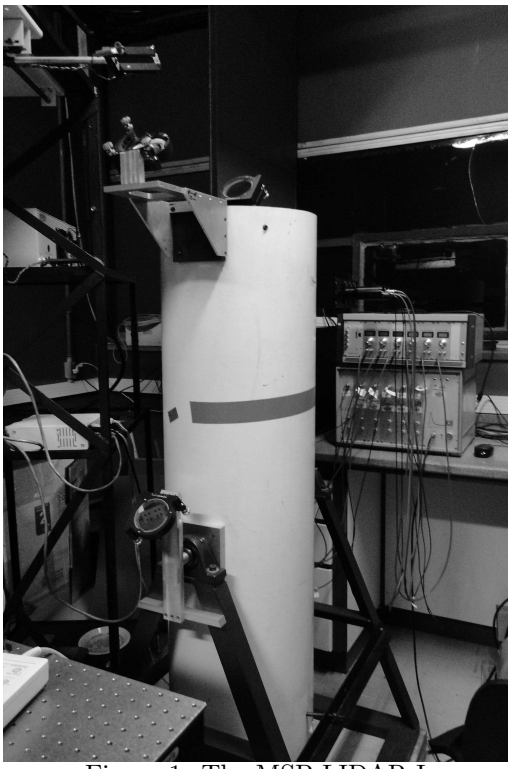

Figure 1: The MSP-LIDAR I

The laser beam has an average diameter of 9 mm and is directed to a beam expander (expands the three wavelengths), which increases the beam diameter about 5 times, with a divergence of less than 0.1 mrad. The expanded laser beam is then directed to the atmosphere through a second set of mirrors (periscope).

A 30 cm diameter telescope (Focal length of 1.5 m) is used to collect the backscattered laser light. The telescope's field of view (FOV) can be adjusted until a desirable value of 0.1 mrad is reached, using a small diaphragm. The

system is currently used with a fixed FOV of 0.1 mrad, which permits a full overlap between the telescope FOV and the laser beam at altitudes higher than 1000m m above the ground level. This FOV value, in accordance with the detection electronics, permits the probing of the atmosphere up to the free troposphere.

The detection box collects the backscattered wavelengths and separates them into 6 different channels (the elastic 355 nm and the corresponding shifted Raman signals: nitrogen 387 nm, and water vapor, 408 nm; the elastic 532 nm and the corresponding shifted Raman signals: nitrogen 607 nm and water vapor 660 nm) using a combination of high-pass and low-pass filters. Each separated beam is directed to narrowbands spectral interference filters (532±1.0 nm FWHM, 355±1.0 nm FWMH, 387±0.25nm FWMH, 408±0.25 nm FWHM, 607±0.25 nm FWHM, 660±0.25 nm FWHM) and then directed to photomultipliers tubes (PMTs). R7400 photomultiplier tubes from Hamamatsu are used for all channels, except for 607 and 660 nm, where R9880U-20 are used. The R9880U-20 has a better quantum efficiency (around 20%) at range 550 - 700 nm, improving the signal to noise ratio of the weak Raman signal at theses wavelengths.

The PMT signals are digitized by a transient recorder TR 20-80/160 for 532 nm, TR 20-160 for 355, 387 and 408 nm, TR 20-40 for 607 and 660 nm, all supplied by LICEL. They are recorded in both analog and photoncounting mode. Corrections of background noise and the dark current are applied before analysis.

In this work, we only use the 355 channel and corresponding Raman channels for water vapor and nitrogen. The reason for this choice is that at this wavelength the atmospheric transmission is higher, improving the signal to noise ratio for the Raman channels.[8] Data were acquired during nighttime (from 21:00 UTC to 00:00 UTC) and integrated every 5 minutes. The vertical spatial resolution is 15 meters.

Table 1: Sumarized Setup of the MSP-LIDAR I

Laser	
Laser type	Nd:YAG Laser (Brilliant B by Quantel)
Wavelengths	355, 532 nm
Pulse energy	230 mJ (355 nm), 400 mJ (532 nm)
Repetition rate	10 Hz
Pulse duration	6 ns
Receiver	
Optical design	30-cm diameter Newtonian telescope
Focal length	1.5 m
Field of view	0.1 mrad
Transient recorder	Licel TR20-80/ TR20-160/ TR20-40
Photoncounting count rate	250 MHz

2.1.2 Radiosoundings

To obtain information about the relative humidity, profile data from radiosounding were used. The soundings (Vaisala RS-92) are launched twice a day, at 12:00 UTC and 00:00 UTC and are distant about 12km from the place where the MSP-LIDAR I is located (Campo de Marte Airport, (−23° 30' S, 46°38' W, 722 m above sea level). From the radiosondings, profiles of temperature and pressure (used to derive RH from LIDAR) can be obtained, and also water vapor mixing ratio profiles, used for calibration of the LIDAR. In this study, data obtained by the 11 September 2012 00:00 UTC sonde were used. Data were available from the University of Wyoming at *weather.uwyo.edu/upperair/sounding.html*.

2.2 Calibration

The methodology to obtain water vapor mixing ratio retrievals from the Raman LIDAR is described in Whiteman at al (1992),[8] Guerrero-Rascado et al. (2008)[9] and Navas-Gusman et al. (2014).[10] The determination of water

vapor mixing ratio (WVMR) profiles is based on the ratio of the Raman signal obtained by water vapor channel and nitrogen channel, applying corrections for atmospheric nitrogen percentage and for differential transmission of the atmosphere in the two scattered wavelengths. As this is a ratio between the two channels (dimensionless), it depends on calibration in order to have access to the real water vapor mixing ratio. Methods for independent calibration using a light source of known spectral characteristics may be used,[11,12] and radiosoundings are widely used when available.[13,14] For 10 September 2012, a WVMR profile obtained from the Campo de Marte Airport 00:00 UTC radiosounding were used for the LIDAR calibration, using an algorithm that compares the WVMR values obtained by the LIDAR with the values obtained by the radiosounding and performs a iterative linear regression.[10] The calibration constant obtained for this particular day is 2.1±0.3 g/kg. At low altitudes, the differences between the LIDAR and the sounding are more expressive, and this difference can arise from the fact the compared profiles are 12 km distant from each other, and inside the the PBL differences can appear in this spatial scales. As altitude increases, the atmosphere is more homogeneous (in horizontal distances), so the agreement is better. Figure 2b shows the percentual deviation of the WVMR values obtained by both instruments, and the mean percent deviation is 6.62%

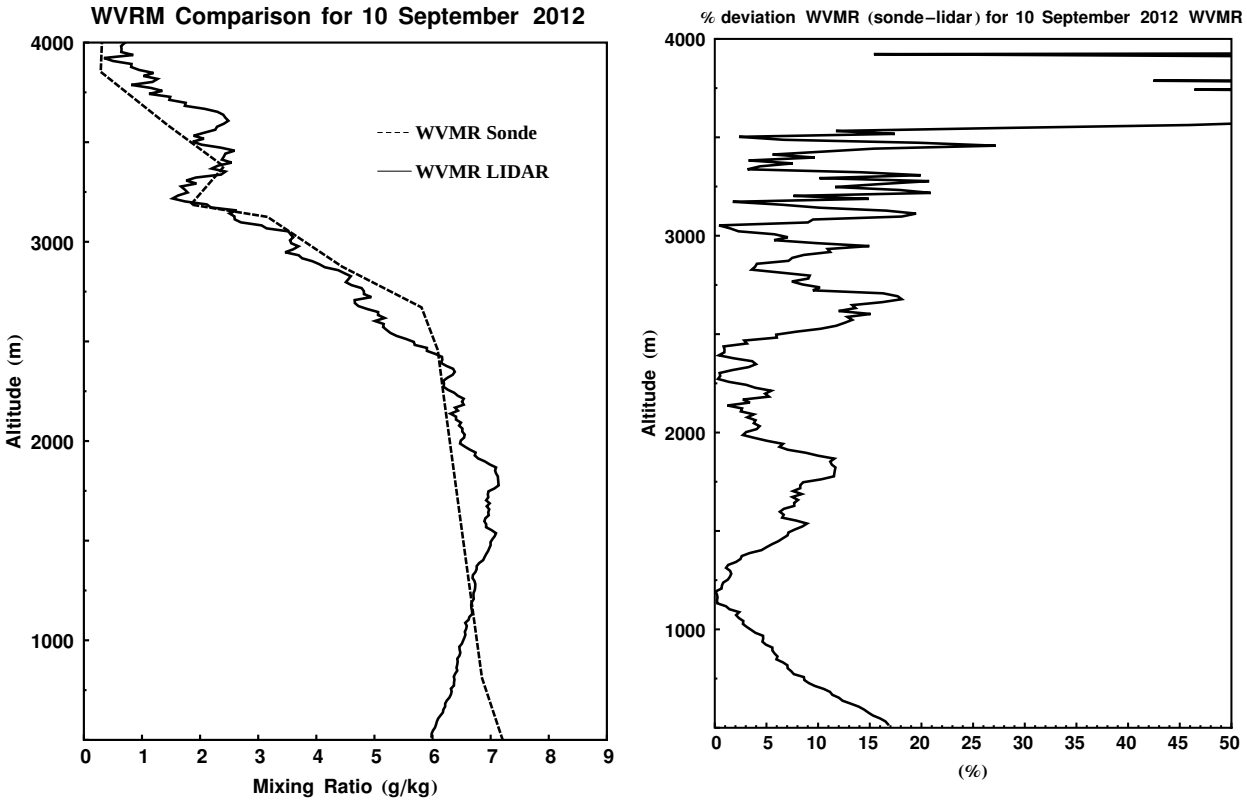

Figure 2: WVMR obtained by the LIDAR after calibration and comparison with the values obtained by the radiosounding. The percentage difference shows that the major differences are in the region where next to the ground and in higher altitudes, where Raman LIDAR signal has a low signal-to-noise ratio

2.3 Obtaining RH profiles using a combination of LIDAR and radiosounding

Computing RH by the combination of the LIDAR and the radiosounding increases the vertical resolution of RH that, in turn, will allow to have more datapoints to perform the computation of hygroscopic growth factor. It also increases the temporal resolution of data since the LIDAR technique allows continuous measurements in time, while the radiosoundings are launched twice a day.The calculation of RH profiles using LIDAR WVMR follows the formulation:[10,15]

$$RH_{(z)} = \frac{E_{(z)}}{E_{w(z)}} \tag{1}$$

where RH is the relative humidity, $E_{(z)}$ is the vapor pressure and $E_{w(z)}$ is the saturation vapor pressure. The vapor pressure is a function of pressure, according to the following equation:

$$E_{(z)} = \frac{P_{(z)} WVMR_{(z)}}{0.622 + WVMR_{(z)}} \tag{2}$$

with P in [Pa] and WVMR in [kg/kg]. The saturation vapor pressure is a function of temperature. There are many empirical formulations to derive saturation vapor pressure,[16] and in this work we used the Hyland-Wexler equation, with T in [K] and P in [Pa]:

$$\log E_{(z)} = \frac{-0.58002206(10^4)}{T} + 0.13914993(10^1) - \frac{0.48640239(10^{-1})}{T} \tag{3}$$
$$+ \frac{0.41764768(10^-4)}{T^2} - \frac{0.14452093(10^{-7})}{T^3} + 0.65459673(10^1)\log(T)$$

In equation 2 and equation 3 pressure and temperature are obtained from the radiosounding.

Figure 3 shows the comparison between the RH profiles obtained by LIDAR and radiosouding. In figure 3b the percentage difference shows a good agreement between both instruments until 2000 m (mean percentage difference 95%). Above this altitude, the differences are large (mean percentage difference 38.6%). This can be explained by the low signal-to-noise ratio of the LIDAR signal at this high)

2.4 Conditions to study hygroscopicity

As described by Veselovskii et al (2009),[7] the ideal condition to evaluate the hygroscopic growth of particles is under a well-mixed atmosphere, with a constant water vapor mixing ratio and potential temperature, and increasing values of RH with altitude. These conditions ensure that any changes in backscattering are due to changes in the size because of water uptake by the particles, and not to changes in the aerosol population. For 10 September 2012, those conditions were verified using data from the radiosounding. Figure 4 shows that the atmosphere presented a constant WVMR and increasing values of RH (from 30% to 70%) from the ground level until approximately 2800m. The same conditions were verified with the LIDAR derived RH and WVMR (figure 5b and figure 5c). Figure 5a shows the vertical backscatter profile measured by the MSP-LIDAR I. It can be seen an increase of the backscatter signal from 1440 to 2800 m.This increase is expected to be from the growth of the aerosol particles by water uptake. It is observed a sharp increase with altitude in the aerosol backscatter coefficient between 1800 and 2430 m, suggesting more intense hygroscopic growth of the aerosol particles.

2.5 The hygroscopic growth factor

The hygroscopic growth factor $\mathbf{f}_\beta(RH)$ ins defined in the following equation:

$$f(RH) = \frac{\beta(RH)}{\beta(RH_{ref})} \tag{4}$$

where all the values of backscatter above a certain height are compared with a reference one. The reference height is chosen at the point with the lowest value of relative humidity in the height range where aerosol hygroscopic growth is expected (i.e. where the backscatter increases with altitude). For 10 September 2012, the reference point was 1560 m, where the relative humidity was equal to 48% (LIDAR) and 45% (sonde), and the cutting edge point was 2400 m, where the RH was 64% both for LIDAR and sonde.

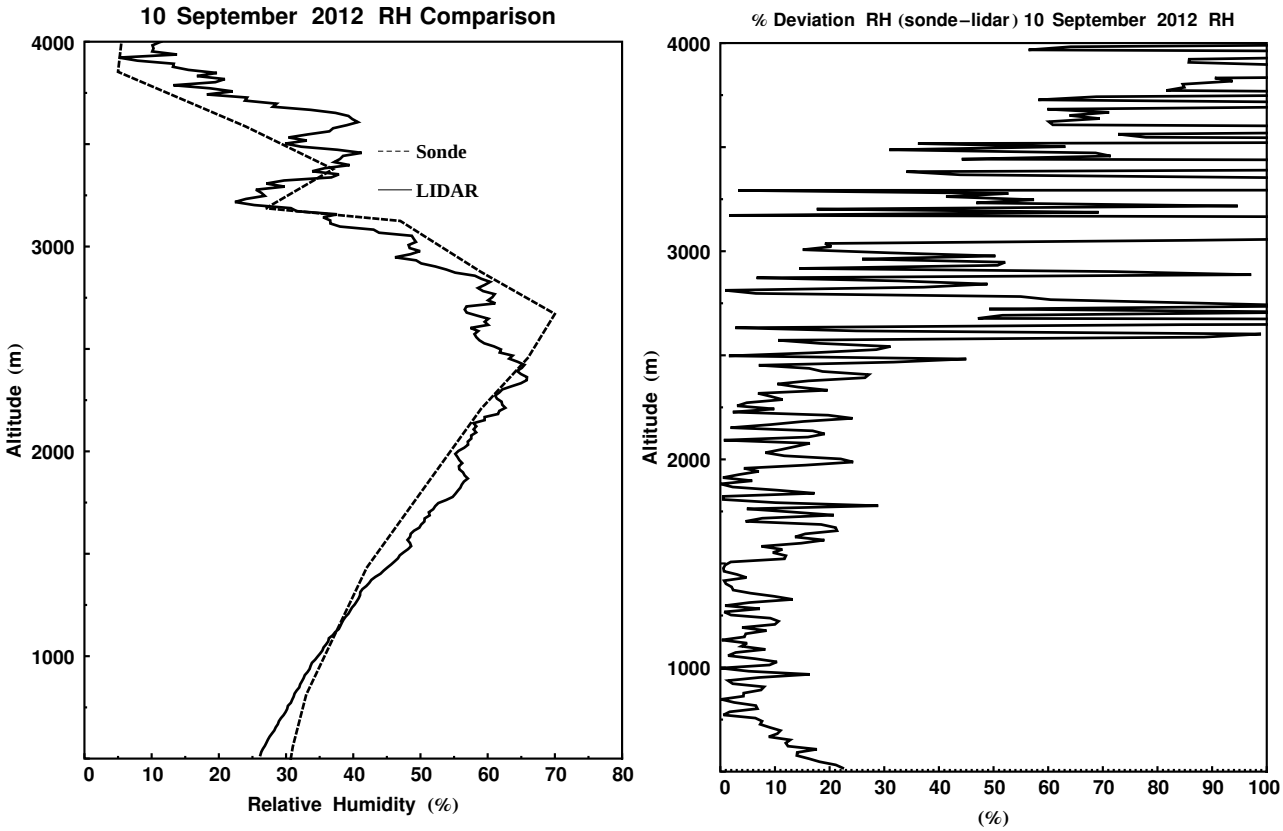

Figure 3: Comparison between the calculated RH obtained by the LIDAR and the radiosounding

There is an empirical parameter that is an estimation of how fast the aerosol population can grow under increasing RH values. This is called the **g** factor,[5,6] and is related to the hygroscopicity of aerosol particles, being larger for more hygroscopic particles.[17,18] Following Hanel (1976),[2] the hygroscopic growth of the aerosol particles can be parametrized, using the equation:

$$\frac{\beta(RH)}{\beta(RH_{ref})} = (\frac{1-RH}{1-RH_{ref}})^{-g} \tag{5}$$

2.6 Normalization

As the range in RH where the hygroscopic growth factor from LIDAR and radiosounding were determined is small, a normalization of $f_\beta(RH)$ using 40% as the reference relative humidity was performed, using equation 4, in order to compare the results to other *in situ* studies (that used 40% RH as the dry condition and 85% as the maximum humidity). The value obtained for **g** without parametrization was used to obtain $f_\beta(40\%)$ and the results of the previous adjustment were divided by this value. Then a new adjustment was performed and $f_\beta(85\%)$ could be calculated. The results are presented in the next section.

3. RESULTS AND DISCUSSIONS

Even if the conditions for hygroscopic growth were present since the ground level, backscattering values started to grow only above 1800 meters. This can be explained because at this point the RH started to be greater than 50% and from previous studies[19] it is known that the growth of the particles is more pronounced in higher levels of relative humidity, specially next to saturation. In this work, the interval of RH where the hygroscopic growth factor could be evaluated is quite small, and it was not possible to verify the growth next to saturation. In this

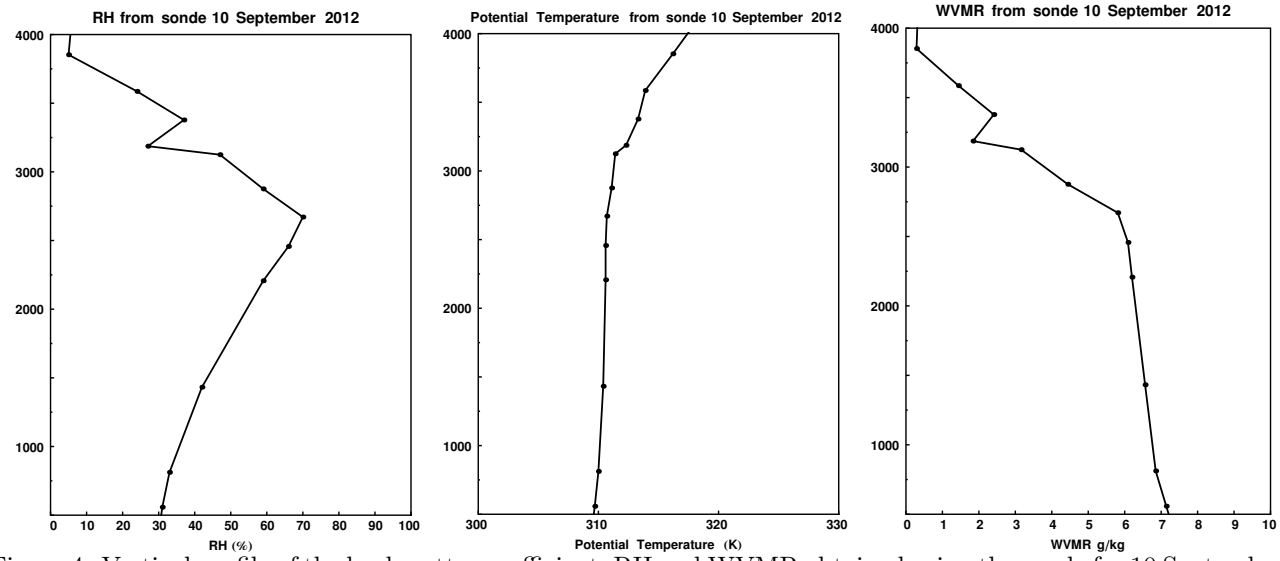

Figure 4: Vertical profile of the backscatter coefficient, RH and WVMR obtained using the sonde for 10 September 2012

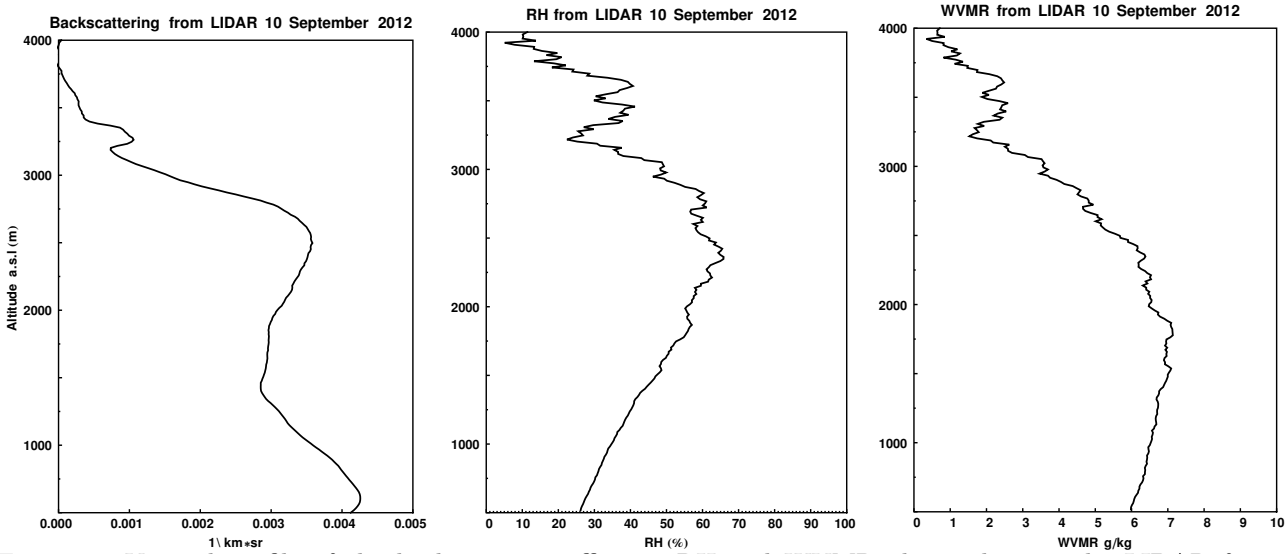

Figure 5: Vertical profile of the backscatter coefficient, RH and WVMR obtained using the LIDAR for 10 September 2012

range, the maximum enhancement was next to 1.2, but the theoretical curve suggests that with this value of **g**, the enhancement would me more than 2 next to the saturation.

The following humidrograms show the hygroscopic curves for 10 September 2012 before and after normalization. Using the normalized function, the $f_\beta(85\%)$ obtained with the LIDAR was 1.58 and the $f_\beta(85\%)$ obtained with the sonde was 1.75

Those values are in agreement with other studies. Zieger at al (2013)[20] found a range of $f_\beta(85\%)$ from 1.28 for Saharan to 3.41 for Artic aerosols. For the **g** factor, Randriamiarisoa et al (2005)[21] found values between 0.47 and 1.35 for urban aerosols over Paris (but using aerosol scattering coefficient instead of backscattering). Gasso et al (2000)[22] reported values between 0.27 and 0.6 for polluted and clean marine aerosols.

During the winter/dry season Metropolitan Area of São Paulo can experience episodes of strong stable layer

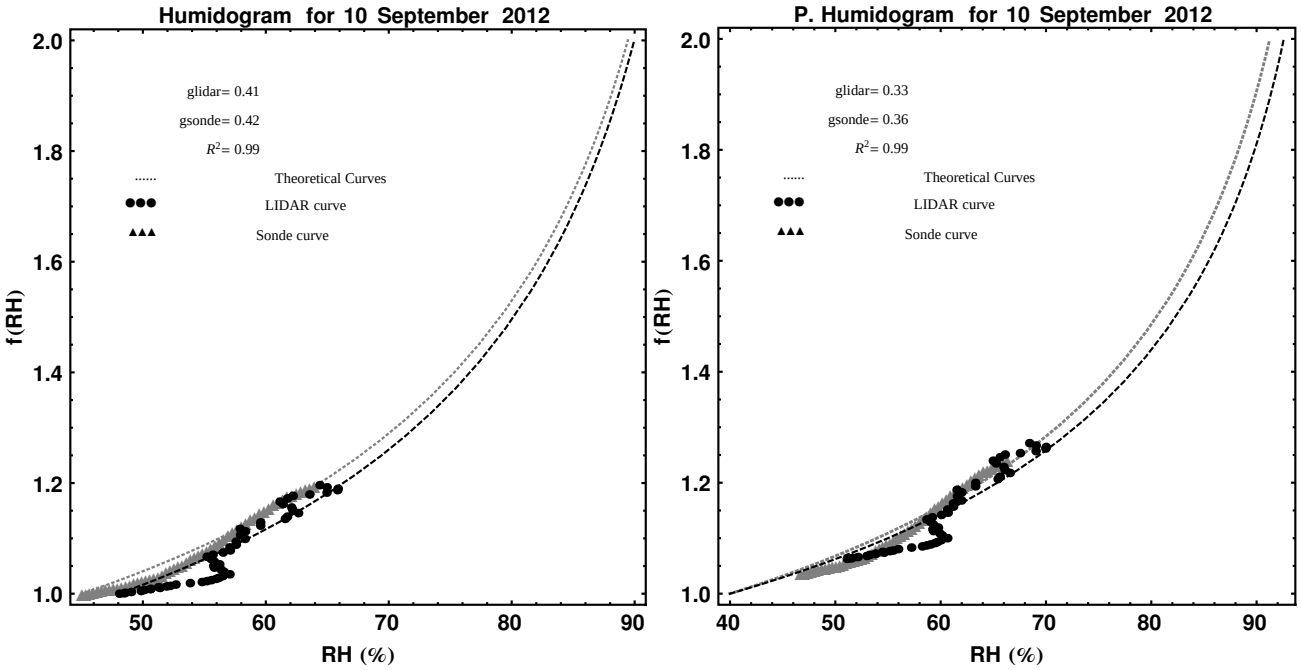

Figure 6: g factor obtained before and after parametrization for LIDAR and sonde for 10 September 2012

between the boundary layer and the free troposphere.[23] Other study indicates the presence of biomass burning aerosol present at the Metropolitan area of São paulo during this period of September of 2012.[24]

The growth factor total uncertainty is very difficult to determine since it is highly dependent on the uncertainties of the aerosol properties and the RH, on the range of RH considered as well as the hygroscopic growth of the particle itself and therefore it is not well characterized yet. Adam et al., (2012) provided estimations based on a sensitivity test and Mie calculations. According to their study, this uncertainty varies between 4% (for RH $\leq$ 40%) and 38% (at RH $\geq$ 95%).[25]

4. CONCLUSION

This work shows that LIDAR system can be a useful tool for measurement of aerosol growth, particularly at high RH levels. Even if there are many uncertainties in the determination of the **g** factor, and to the best of our knowledge never in the literature a study was performed with enough cases to have statistics using the LIDAR, this study shows an application of this technique. Also, other instruments could be applied in synergy with the LIDAR system to help to help with the determination of optical parameters (such as sunphotometer) or chemical composition.

5. ACKNOWLEDGMENTS

This work was supported by FAPESP (Fundação da Amparo à Pesquisa do Estado de São Paulo) through the project 2009/14758-7, the Posdoctoral project 2011/14365-5 and the thematic project 2008/58104-8;

Thanks to Igor Veselovskii and David Whiteman from NASA Goddard Space Flight Center for the important contribution in data analysis

REFERENCES

[1] P. Rodrigues, F. Lopes, R. F. Costa, W. Nakaema, and E. Landulfo, "Indirect aerosol hygroscopic growth observations with a backscatter LIDAR," in *Proceedings of SPIE*, **7832**, p. 78320F, SPIE Digital Library, 2010.

[2] G. Hänel, "The properties of atmospheric aerosol particles as functions of the relative humidity at thermodinamic equilibrium with the surrounding moist air," *Advances in Geophysics* **19**, pp. 73–188, 1976.

[3] P. Rodrigues, F. Lopes, R. F. Costa, W. Nakaema, and E. Landulfo, "Indirect aerosol hygroscopic growth observations with a backscattering lidar, part ii: Five day breeze onset data analyses," in *Proceedings of SPIE*, **8182**, p. 81820Y, SPIE Digital Library, 2011.

[4] B. Svenningsson, J. Rissler, E. Swietlicki, M. Mircea, M. Bilde, M. Facchini, S. Decesari, S. Fuzzi, J. Zhou, J. Monster, and T. Rosenorn, "Hygroscopic growth and critical supersaturations for mixed aerosol particles of inorganic and organic compounds of atmospheric relevance," *Atmospheric Chemistry and Physics* **6**, pp. 1937–1952, 2006.

[5] R. Kotchenruther and P. Hoobs, "Humidification factors of aerosols from biomass burning in Brazil," *Journal of Geophysical Research* **104**, pp. 32081–32089, 1998.

[6] R. Kotchenruther, P. Hoobs, and D. Hegg, "Humidification factors for atmospheric aerosols off the mid-atlantic coast of the united states," *Journal of Geophysical Research* **104**, pp. 2239–2251, 1999.

[7] I. Veselovskii, D. Whiteman, A. Kolgotin, E. Andrews, and M. Korenskii, "Demosntration of aerosol property profiling by multiwavelength LIDAR under varying relative humidity conditions," *Journal of Atmospheric and Oceanic Technology* **26**, pp. 1543–1557, 2009.

[8] D. N. Whiteman, S. Melfi, and R. Ferrare, "Raman lidar system for the measurement of water vapor and aerosols in the earths atmosphere," *Applied Optics* **31**, pp. 3068–3082, 1992.

[9] J. L. Guerrero-Rascado, B. Ruiz, G. Chourdakis, G. Georgoussis, and L. Alados-Arboledas., "One year of water vapour raman lidar measurements at the andalusian centre for environmental studies (CEAMA)," *International Journal of Remote Sensing* **29**, pp. 5437–5453, 2008.

[10] F. Navas-Gusman, J. Fernandes-Galvez, M. Granados-Munhoz, J. Bravo-Aranda, and L. Alados-Arboledas., "Tropospheric water vapor and relative humidity profiles from lidar and microwave radiometry.," *Atmospheric Measurements Techniques* **7**, pp. 1201–1211, 2014.

[11] D. D. Venable, D. N. Whiteman, M. N. Calhoun, A. O. Dirisu, R. M. Connell, and E. Landulfo, "Lamp mapping technique for independent determination of the water vapor mixing ratio calibration factor for a raman lidar system," *Applied Optics* **40**, pp. 4622–4632, 2011.

[12] E. Landulfo, R. F. Da Costa, A. S. Torres, F. J. S. Lopes, D. N. Whiteman, and D. D. Venable, "Raman water vapor lidar calibration," *Proc. SPIE* **7479**, pp. 74790J–74790J–9, 2009.

[13] A. Moss, R. J. Sica, E. McCullough, K. Strawbridge, K. Walker, and J. Drummond, "Absolute accuracy of water vapor measurements from six operational radiosondes types launched during AWEX-G and implications for AIRS validation," *Atmospheric Measurement Techniques* **6**, pp. 741–749, 2006.

[14] T. Leblanc and I. S. McDermid, "Accuracy of raman lidar water vapor calibration and its applicability to long-term measurements," *Applied Optics* **47**, pp. 5592–5603, 2008.

[15] I. Mattis, A. Ansmann, D. Althausen, V. J. andU. Wandinger, D. Muller, Y. F. Arshinov, S. M. Bobrovnikov, and I. B. Serikov, "Relative-humidity profiling in the troposphere with a Raman LIDAR," *Applied Optics* **41**, pp. 6451–6462, 2002.

[16] H. Vomel, "The columbus navigation homepage," 2013.

[17] V. Wulfmeyer and G. Feingold, "On the relationship between relative humidity and particle backscattering coefficient in the marine boundary layer determined with differential absorption lidar," *Journal of Geophysical Research* **105(D4)**, pp. 4729–4741, 2000.

[18] G. Feingold and B. Morley, "Aerosol hygroscopic properties as measured by lidar and comparison with in situ measurements," *Journal of Geophysical Research* **108**, p. 4327, 2003.

[19] R. Tardif, "Boundary layer aerosol backscattering and its relatioship to relative humidity from a combined raman-elastic backscattering LIDAR," 2002.

[20] P. Zieger, R. Fierz-Schmidhauser, E.Weingartner, and U. Baltensperger, "Effects of relative humidity on aerosol light scattering: results from different european site," *Atmospheric Chemistry and Physics Discussions* **13**, pp. 8939–8984, 2013.

[21] H. Randriamiarisoa, P. Chazette, P. Couvert, J. Sanak, and G. Megie, "Relative humidity impact on aerosol parameters in a paris suburban arear," *Atmos. Chem. Phys. Discuss.* **5**, pp. 8091–8147, 2005.

[22] S. Gasso, "Influence of humidity on the aerosol scattering coefficient and its effect on the upwelling radiance during ace-2," *Tellus* **52B**, pp. 546–5673, 2000.

[23] E. Landulfo and F. J. S. Lopes, "Initial approach in biomass burning aerosol transport tracking with calipso and modis satellites, sunphotometer and a backscatter lidar system in Brazil," *Proc. SPIE* **7479**, pp. 74790J–74790J–9, 2009.

[24] F. J. S. Lopes, G. A. Moreira, P. F. Rodrigues, J. L. Guerrero-Rascado, M. F. Andrade, and E. Landulfo, "Lidar measurements of tropospheric aerosol and water vapor profiles during the winter season campaigns over the metropolitan area of são paulo - brazil.," *Proc. SPIE* **IN PRESS**, 2014.

[25] M. Adam, J. P. Putaud, S. M. dos Santos, A. Dell'Acqua, and C. Gruening, "Aerosol hygroscopicity at a regional background site (ispra) in northern italy," *Atmos. Chem. Phys. Discuss.* **12**, p. 5703–5717, 2012.